Materials Transactions, Vol. 44, No. 4 (2003) pp. 705 to 708

Effect of Sodium Hypophosphite on the Structure and Properties of Electrodeposited Ni–W–P Alloys

Jamil Ahmad*, Katsuhiko Asami, Akira Takeuchi and Akihisa Inoue

Institute of Materials Research (IMR), Tohoku University, Sendai 980-8577, Japan

Amorphous and nanocrystalline Ni–W–P alloy films have been prepared by electrodeposition. The effect of sodium hypophosphite in the bath is important in determining the W and P contents of the alloy. The alloys prepared in the bath containing more than about 0.15 mol/L of sodium hypophosphite are only Ni–P alloys containing high P contents (>21% (at)) and no W at all. However, as the sodium hypophosphite content is decreased, the W content in the alloy increases and reaches about 20% (at) with decreasing P content to about 1% (at) at 6×10^{-4} mol/L of sodium hypophosphite. The alloys containing high P contents are amorphous, while those containing high W contents have a nanocrystalline phase with apparent grain size of 2.3 nm at 20% (at) W content. These nanocrystalline alloys show high hardness values up to about 780 MVH.

(Received December 11, 2002; Accepted February 26, 2003)

Keywords: *nickel–tungsten–phosphorus alloys, electrodeposited, sodium hypophosphite, amorphous, nanocrystalline*

1. Introduction

In the last two decades, amorphous and nanocrystalline alloys have emerged as promising alloys with novel mechanical,[1–3] magnetic[4–7] and catalytic[8–11] properties and excellent corrosion resistance.[12–17] These alloys have been largely developed by rapid solidification and physical vapor deposition techniques. However, electrodeposition is an alternative technique, which is not only less expensive, but also very versatile and easily adaptable for industrial applications. That is why it has found successful applications for the production of amorphous and nanocrystalline alloys on industrial scale. A recent example is the in-situ repair of nuclear steam generator in Toronto by electrodepositing nanocrystalline nickel.[18]

A special advantage of electrodeposition is that we can produce alloys having elements with very high melting temperature, such as W, at room temperature and normal atmosphere. Among such alloys amorphous and nanocrystalline Ni–W and Ni–W–P alloys are of special interest for their excellent mechanical properties.

Recently Yamasaki *et al.*[19,20] has produced Ni–W amorphous and nanocrystalline alloys by electrodeposition. These alloys show very good mechanical properties and may replace hard chromium films, which are of great concern for the industrialists because of their environmentally hazardous baths. However, Ni–W alloys have high internal stress, which is main hindrance in their use on industrial scale.

Amorphous Ni–W–P alloys have mostly been produced by electroless deposition. We could find only one reference for electrodeposited Ni–W–P amorphous alloys[21] and there is perhaps no report on the electrodeposited nanocrystalline Ni–W–P alloys.

In the present work we produced amorphous and nanocrystalline Ni–W–P alloys by electrodeposition. For this we used sodium hypophosphite in the electroplating bath. It was found that W and P contents of the alloy were sharply dependent on the sodium hypophosphite content of the bath, while the structure of the alloy was dependent on the P and W contents of the alloy.

*Corresponding author: mirza@imr.tohoku.ac.jp

2. Experimental

The bath composition and the conditions used for the electrodeposition are shown in Table 1. The bath is similar to that used by Yamasaki *et al.* for the preparation of Ni–W alloys, except that sodium hypophosphite was added to it to introduce P in the deposited alloys. For electroplating, copper plates of dimensions 0.5 mm × 15 mm × 10 mm were used as substrate. Before electroplating they were electrocleaned in an alkaline solution and then electropolished in an acidic solution. Platinum electrode was used as counter electrode. Potential was measured against saturated calomel electrode (SCE). Constant current was applied by Hokuto Denko HZ-3000 power unit. The temperature of the bath was controlled by a thermostat. The initial pH value was maintained between 8.92 and 8.97. However, it was found that pH changed during the electroplating and at the end of experiment lied in the range of 8.27 to 8.37.

The amorphous and nanocrystalline structures were identified by x-ray diffraction (XRD). The film thickness (30–50 μm) was sufficient to avoid the appearance of substrate

Table 1 Composition and operating conditions of the electroplating bath.

Basic Bath Composition	
$NiSO_4 \cdot 6H_2O$	0.06 mol/L
$Na_3C_6H_5O_7 \cdot 2H_2O$	0.5 mol/L
$Na_2WO_3 \cdot 2H_2O$	0.14 mol/L
NH_4Cl	0.5 mol/L
NaBr	0.15 mol/L
$NaH_2PO_2 \cdot H_2O$	0.0006–0.1487 mol/L
Operating Conditions	
Temperature	348 K
Time	3.6 ks
pH	8.92–8.97
Current density	2.0 kA/m^2

peak in the diffraction graph. Apparent grain size was calculated from the full width half maximum (FWHM) of XRD peaks. To examine the thermal stability of the amorphous alloys, differential scanning calorimetry (DSC) was performed using Seiko SII-320 DSC system. Compositional analysis was performed by scanning electron microscopy (SEM: Hitachi S-800) equipped with Kevex energy dispersive spectroscopy (EDS) system. The mechanical properties were measured with a Vicker's hardness tester under a load of 50 g.

3. Results and Discussion

Figure 1 shows the effect of sodium hypophosphite on the P and W contents of the alloy. It is observed that the tungsten content of the alloy is sharply dependent on the sodium hypophosphite content of the bath. A negligible amount of tungsten is obtained in the alloy when the sodium hypophosphite content is greater than 8×10^{-2} mol/L. As the sodium hypophosphite content is decreased, the W content of the alloy increases. It is also seen in Fig. 1 that the slope of the curve between tungsten content and sodium hypophosphite content increases with a decrease in the sodium hypophosphite content, such that at very low sodium hypophosphite contents of the bath, the tungsten content is sensitive to the sodium hypophosphite content. A slight change in the sodium hypophosphite content of the bath below 9.3×10^{-3} mol/L results in a sharp change in the tungsten content of the alloy. Exactly opposite behavior is observed for the phosphorus content. At lower contents of sodium hypophosphite, the phosphorus content increases sharply with an increase in the sodium hypophosphite content, but it tends to saturate, when sodium hypophosphite content increases beyond 4×10^{-4} mol/L.

Sodium citrate and ammonium chloride are added to the Ni–W plating bath as a complexing agent for the induced co-deposition of tungsten with nickel. However, as observed here, the effect of sodium hypophosphite is just opposite to it. It hinders the co-deposition of tungsten with nickel. However, very small amounts of sodium hypophosphite are useful for the introduction of phosphorus in these alloys. The composition of the alloys can be controlled by making very slight variations in the sodium hypophosphite content of the bath. Such a bath, therefore, needs very careful control in order to get reproducible results.

Figure 2 shows the effect of sodium hypophosphite on the structure of the alloys. X-ray diffraction patterns of only four alloys have been shown. It is observed that the width of the XRD peak of the deposited alloys increases with an increase in the sodium hypophosphite content of the bath. It appears that the structure is nanocrystalline at lower sodium hypophosphite contents and becomes amorphous as the sodium hypophosphite content is increased. Figure 3 shows the apparent grain size of the deposited alloys as a function of sodium hypophosphite content in the bath. The apparent grain size was determined from the XRD peaks by using the following Scherrer's formula.

$$B = (0.94\lambda)/(D\cos\theta)$$

where

λ = wavelength of the X-ray used

θ = diffraction angle

D = grain size and

B = FWHM of XRD peak (rad)

The feature of Fig. 3 is similar to that of Fig. 1. There is a sudden drop in the apparent grain size from 8.1 nm for the

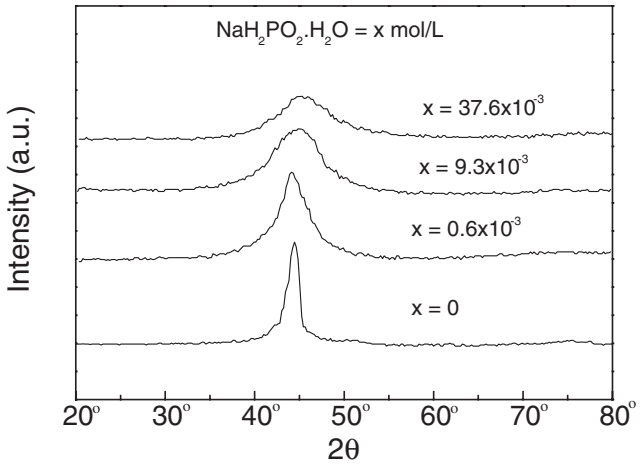

Fig. 2 X-ray diffraction patterns of alloys deposited at various concentrations of sodium hypophosphite in the plating bath.

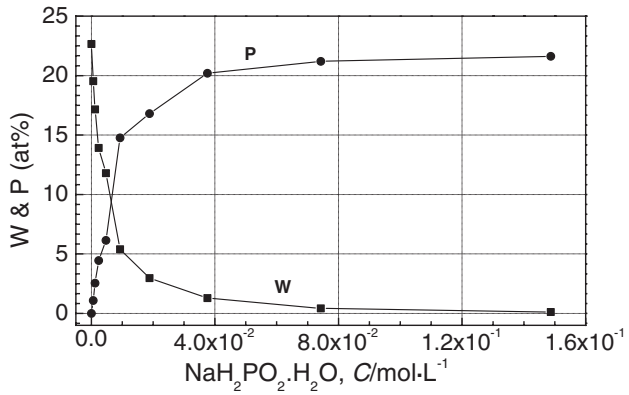

Fig. 1 Effect of sodium hypophosphite on the tungsten and phosphorus contents of the electrodeposited nickel–tungsten–phosphorus alloys.

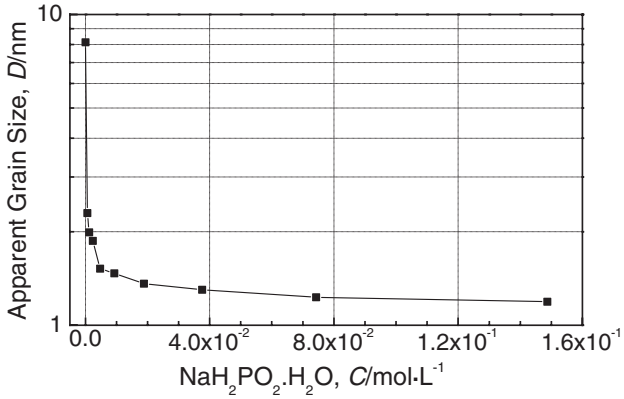

Fig. 3 Apparent grain size of alloys deposited at various concentrations of sodium hypophosphite, calculated from the X-ray diffraction peaks.

alloy containing no phosphorus to 2.3 nm for the alloy containing only 1% (at) phosphorus. Then as the phosphorus content increases, the apparent grain size decreases. At lower sodium hypophosphite contents, where the phosphorus content increases rapidly, the apparent grain size falls down rapidly. When phosphorus content tends to saturate at higher sodium hypophosphite contents, the apparent grain size also remains almost constant. It may reflect the formation of amorphous phase in high phosphorus containing alloys. The presence of amorphous phase was confirmed by DSC.

Figure 4 shows the DSC curves of the alloys deposited at different contents of sodium hypophosphite. The alloys deposited in solutions containing more than 9.3×10^{-3} mol/L sodium hypophosphite show two distinct crystallization peaks. The first peak appears in the temperature range of 605 to 687 K and the second one in the range of 720 to 790 K. The crystallization temperature corresponding to both peaks increases with an increase in the tungsten content of the alloy. It shows that the thermal stability of the amorphous Ni–W–P alloys increases with increasing tungsten content of the alloys. However, when the sodium hypophosphite content decreases to below 9.3×10^{-3} mol/L, which corresponds to about 11% (at) tungsten content of alloy, no peak is observed, showing that the alloy is no more amorphous but nanocrystalline.

Deposition rate of the alloys is also affected by the sodium hypophosphite content of the bath. As shown in Fig. 5, the deposition rate decreases with an increase in the sodium hypophosphite in the bath. The deposition rate for the alloy deposited from the bath containing 6×10^{-4} mol/L sodium hypophosphite is about 2.02×10^{-4} kg/m^2/s and it decreases to about 1.09×10^{-4} kg/m^2/s for the alloy deposited from solution containing 14.9×10^{-2} mol/L sodium hypophosphite. In other words, the alloys containing higher tungsten and lower phosphorus content have higher deposition rates as compared to those containing higher phosphorus and lower tungsten content.

Figure 6 shows the Vicker's microhardness of the deposited alloy films as a function of sodium hypophosphite content of the bath. The hardness of the films decreases with an increase in the sodium hypophosphite content. This seems

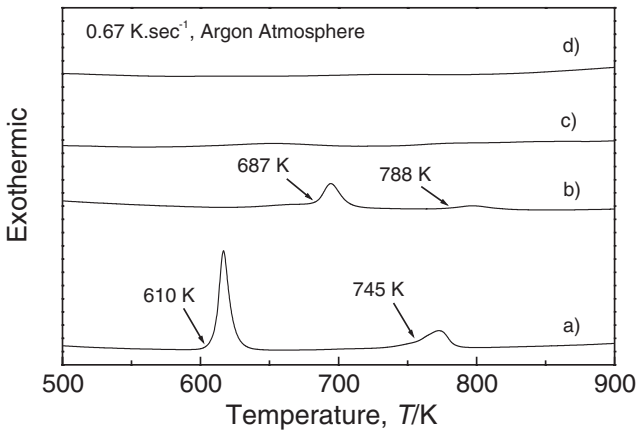

Fig. 4 DSC curves of alloys deposited at different concentrations of sodium hypophosphite; a) 0.0376 mol/L, b) 0.0093 mol/L, c) 0.0047 mol/L, d) 0.0006 mol/L.

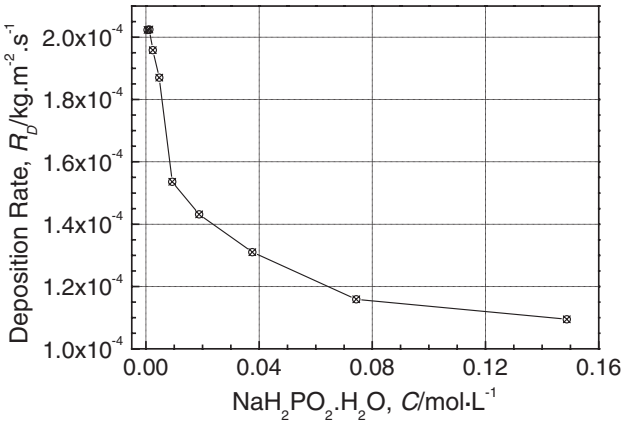

Fig. 5 Effect of sodium hypophosphite on the deposition rate of the electrodeposited alloys.

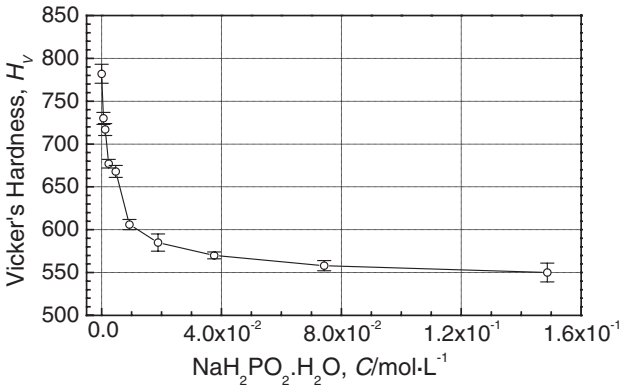

Fig. 6 Effect of sodium hypophosphite on the hardness of the deposited alloys.

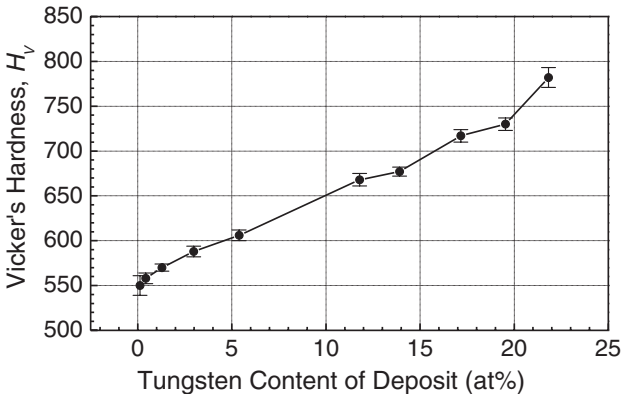

Fig. 7 Relationship between tungsten content and hardness of the electrodeposited alloys.

to be associated with the tungsten content of the alloys. Figure 7 shows the relationship between tungsten content and hardness of the electrodeposits. Hardness increases somewhat linearly with increase in tungsten content. The alloys containing higher tungsten content show higher hardness values and as the tungsten content decreases, hardness also decreases. Figure 8 shows the relationship between hardness and grain sizes of the alloys. It is observed that hardness decreases slowly when grain size decreases

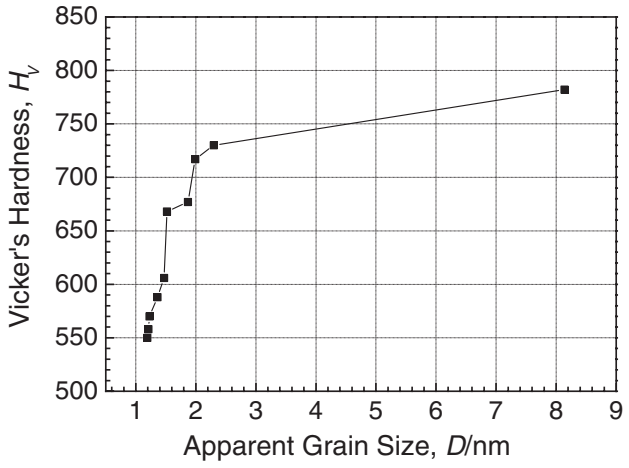

Fig. 8 Relationship between apparent grain size and hardness of the electrodeposited alloys.

from 8 to 2.2 nm, while it decreases sharply as the grain size decreases from 2.2 to 1.1 nm. Yamasaki *et al.* has shown that Ni–W based alloys show decrease in hardness with decrease in grain size when the grain size is less than 10 nm. It is due to the increase in intercrystalline volume fraction of alloys at such lower grain sizes. Accordingly, if there is no significant change in grain size, change in hardness should also be negligible. This is just opposite to what we observe in Fig. 8. Therefore, the change in hardness is due to change in tungsten content of the alloy and not because of change in grain size or structure.

It must be noted that all these amorphous and nanocrystalline alloys show brittleness due to hydrogen absorption during the deposition process.

4. Conclusions

(1) Sodium hypophosphite, when introduced in Ni–W deposition bath, inhibits the co-deposition of tungsten with nickel. However, when used in very small quantities, it can be used to produce Ni–W–P alloys. The alloy composition is sensitive to sodium hypophosphite content of the bath. Therefore, bath composition should be controlled carefully.

(2) The grain size of the Ni–W–P alloys decreases with increasing phosphorus content and the alloys become amorphous when the phosphorus content increases beyond about 5% (at).

(3) The thermal stability of the amorphous alloys increases with increasing tungsten content of the amorphous alloys.

(4) Deposition rate and hardness of the deposited alloys decrease with an increase in the sodium hypophosphite content of the electroplating bath. The decrease in hardness is due to the decrease in the tungsten content of the alloys.

REFERENCES

1) T. Zhang and A. Inoue: Mater. Trans. **43** (2002) 708–711.
2) A. Inoue, M. Matsushita, Y. Kawamura, K. Amiya, K. Hayashi and J. Koike: Mater. Trans. **43** (2002) 580–584.
3) A. Inoue, Y. Kawamura, M. Matsushita and K. Hayashi: Mater. Sci. Forum. **386** (2002) 509–517.
4) A. Inoue and BL. Shen: Mater. Trans. **43** (2002) 766–769.
5) BL. Shen, H. Kimura and A. Inoue: Mater. Trans. **43** (2002) 589–592.
6) H. Koshiba and A. Inoue: Mater. Trans. **42** (2001) 2572–2575.
7) BL. Shen, H. Koshiba, A. Inoue, H. Kimura and T. Mizushima: Mater. Trans. **42** (2001) 2136–2139.
8) H. Habazaki, M. Yamasaki, A. Kawashima and K. Hashimoto: Appl. Organomet. Chem. **14** (2000) 803–808 (Sp. Iss. SI).
9) M. Yamasaki, H. Habazaki, K. Asami and K. Hashimoto: J. Electrochem. Soc. **147** (2000) 4502–4506.
10) M. Yamasaki, M. Komori, E. Akiyama, H. Habazaki, A. Kawashima, K. Asami and K. Hashimoto: Mat. Sci. Eng. A-Struct. **267** (1999) 220–226.
11) H. Habazaki, T. Yoshida, M. Yamasaki, M. Komori, K. Shimamura, E. Akiyama, A. Kawashima and K. Hashimoto: Stud. Surf. Sci. Catal. **114** (1998) 261–266.
12) S. Pang, T. Zhang, K. Asami and A. Inoue: Mater. Trans. **43** (2002) 2137–2142.
13) S. Pang, T. Zhang, K. Asami and A. Inoue: Mater. Trans. **43** (2002) 1771–1773.
14) S. Pang, T. Zhang, K. Asami and A. Inoue: Corros. Sci. **44** (2002) 1847–1856.
15) M. Mehmood, B.-P. Zhang, E. Akiyama, H. Habazaki, A. Kawashima, K. Asami and K. Hashimoto: Corros. Sci. **40** (1998) 1–17.
16) M. Mehmood, E. Akiyama, H. Habazaki, A. Kawashima, K. Asami and K. Hashimoto: Corros. Sci. **41** (1999) 1871–1890.
17) M. Mehmood, E. Akiyama, H. Habazaki, A. Kawashima, K. Asami, K. Hashimoto: Corros. Sci. **42** (2000) 361–382.
18) G. Palumbo, F. Gonzalez, A. M. Brennenstuhl, U. Erb, W. Shmayda and P. C. Lichtenberger: Nanostructured Materials **9** (1997) 737–746.
19) T. Yamasaki, R. Tomohira, Y. Ogino, P. Schlobmacher and K. Ehrlich: Plating and Surface Finishing **87** (2000) 148–152.
20) T. Yamasaki, P. Schlobmacher, K. Ehrlich and Y. Ogino: Nanostructured Materials **10** (1998) 375–388.
21) S. Yao, S. Zhao, H. Guo and M. Kowaka: Corrosion **52** (1996) 183–186.